Phytotaxa 305 (3): 165–178
http://www.mapress.com/j/pt/

Article

ISSN 1179-3155 (print edition)
PHYTOTAXA
ISSN 1179-3163 (online edition)

https://doi.org/10.11646/phytotaxa.305.3.4

A re-investigation of three Frenguelli's *Caloneis* taxa (Pinnulariaceae, Bacillariophyta) from Argentina

INES SUNESEN[1, 2], JONAS A. TARDIVO KUBIS[1] & EUGENIA A. SAR[1, 2]
[1]*División Ficología, Facultad de Ciencias Naturales y Museo, Paseo del Bosque s/n, 1900 La Plata, Argentina*
[2]*CONICET*
Correspondence author: easar@fcnym.unlp.edu.ar

Abstract

Caloneis mendosina var. *mendosina*, *Caloneis mendosina* var. *minor* and *Caloneis quilinensis* from slides of the Frenguelli Collection deposited at the Herbarium of the División Ficología 'Dr. Sebastián A. Guarrera' (LPC), were investigated using light microscope (LM). Unmounted material related to these slides was observed using the scanning electron microscope (SEM). Specimens of both varieties of *C. mendosina* found in the original material show a continuous range of size and stria density, and are ultrastructurally similar; thus the taxa are considered conspecific. Specimens of *C. quilinensis* found in the original material show more variability than described in the protologue. A continuous range of size, stria density, shape of the frustules and valve outline was observed between *C. mendosina* and *C. quilinensis*. Additionally, ultrastructural comparison of both taxa showed numerous features in common including shape of the valve surface, morphology of the valve mantle, shape of the axial area, shape of the fascia, position of the raphe, morphology and orientation of the external central and distal raphe fissures, and size and position of the elliptical apertures of the alveolate striae. The evidence that there is no morphologic and morphometric discontinuity between these Frenguelli taxa and that they come from similar diatomaceous earth deposits, justify considering them conspecific. Based on the principle of priority the correct name of the species is *Caloneis mendosina*. The description of *C. mendosina* was emended, a lectotype slide was selected, and a comparison with some allied species was conducted.

Key words: *Caloneis quilinensis*, *Caloneis mendosina* var. *mendosina*, *Caloneis mendosina* var. *minor*, fine morphology, lectotypification

Introduction

Caloneis mendosina Frenguelli and *C. mendosina* var. *minor* Frenguelli from the Guayquerías (Province of Mendoza, Argentina) and *C. quilinensis* Frenguelli from Quilino (Province of Córdoba, Argentina) were erected as presumptively fossil taxa. These taxa show morphological similarities and were found in earth deposits accompanied by two predominant, abundant or frequent species, *Rhopalodia argentina* (Brun) O. Müller (Frenguelli 1934: 365) [which correct name according with VanLandingham (1978: 3609) is *Rhopalodia gibberula* var. *argentina* (Brun) Frenguelli (1923: 76, pl. 1, figs 28, 29)] and *Denticula valida* (Pedicino) Grunow in Van Heurck (1881: pl. 49, fig. 5).

Frenguelli (1934: 351, pl. 1, figs 9–11 and fig. 12) described *Caloneis mendosina* and *C. mendosina* var. *minor* based on samples collected from the Pleistocene diatomaceous earth deposit at Guayquerías; however no type material was designated. Both taxa were found in one of the two series obtained from the intercalations located at different levels of the upper half of the Araucaniano, in the "guaycos" of the Seco del Agua Salada River. According to the Table presented by Frenguelli (1934: 341–343) these taxa were accompanied by several freshwater species with a preference for shallow clean water with a high saline concentration.

Frenguelli in Frenguelli & Cordini (1937: 96, 104, pl. 3, figs 14–18) described *Caloneis quilinensis* based on samples collected in the diatomaceous earth deposits from Quilino that were very recent depositions, probably Holocene in age; however without designating the type material. The taxon was found in three series obtained from the profile of the trench placed along the way connecting San Pedro Norte to Quilino, with different relative abundances. According to the Table presented by Frenguelli (in Frenguelli & Cordini 1937: 86–88) *C. quilinensis* was accompanied by several freshwater species with a preference for shallow waters in swampy areas. Additionally, Frenguelli & Cordini (1937:

Accepted by PAUL B. HAMILTON: 2 Apr. 2017; published: 28 Apr. 2017

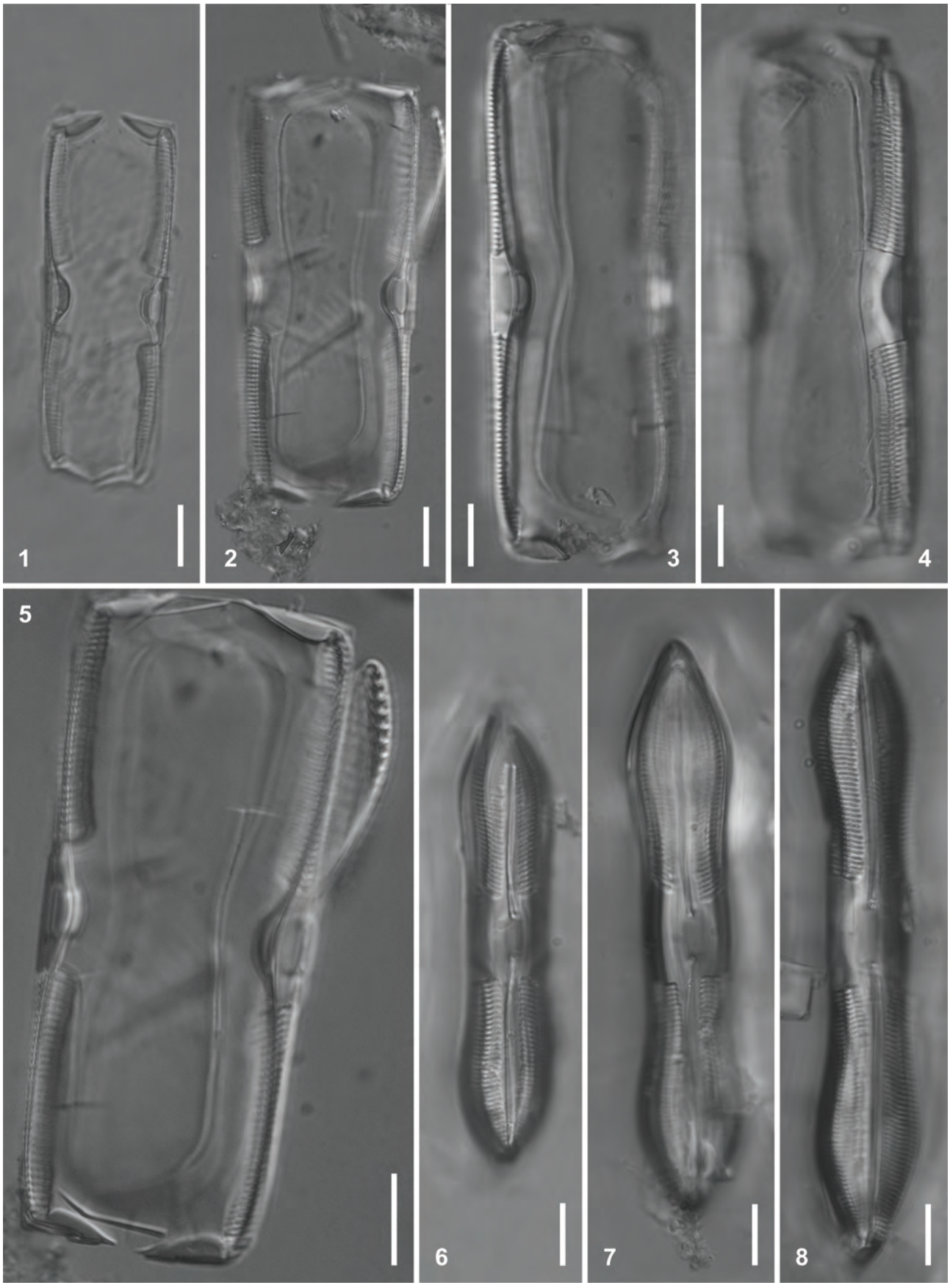

FIGURES 1–8. *Caloneis mendosina* Frenguelli (emend. Sar & Sunesen) from syntype material of *C. mendosina* and *C. mendosina* var. *minor*. LM. 3, 4, 7, 8, Lectotype slide. Figs 1–5. Frustules in girdle view, note obliquely reinforced corners. Figs 6–8. Valves linear-panduriform in outline. Note broad fascia and radiate striation throughout the valve. Scale bars: 10 µm.

109) analyzed a sample of living material collected from submerged plants and decaying plant residues from the bottom of the trench, establishing that the diatom flora was similar to that in the sediments with differences in the relative abundance; however *C. quilinensis* was not present.

As far as we can determine there has been no additional records of *Caloneis mendosina*, *C. mendosina* var. *minor* and *C. quilinensis* reported as extinct or extant until now.

In the present study, we examined original material with these three taxa in light microscopy and because unmounted material was available from the Frenguelli Collection (Sar *et al*. 2009: 82, Table 1) we also studied them with scanning electron microscopy.

The aims of this study are to give a comprehensive description and comparison of the studied taxa, to compare them with morphologically similar species, and finally, to propose the necessary taxonomic-nomenclatural changes.

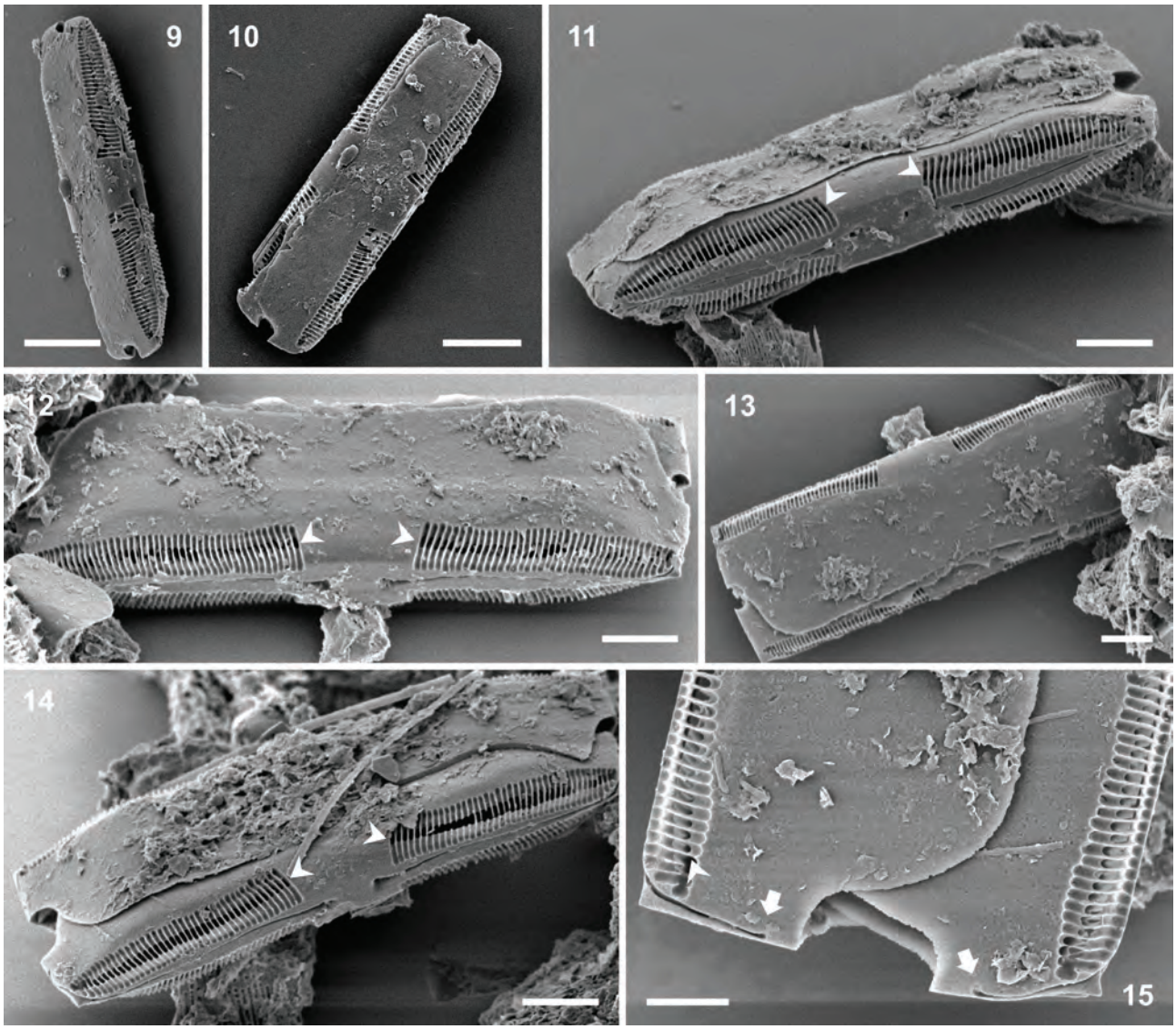

FIGURES 9–15. *Caloneis mendosina* Frenguelli (emend. Sar & Sunesen) from unmounted syntype material of *C. mendosina* and *C. mendosina* var. *minor*. SEM. Arrowheads show the internal aperture of the alveolate areolae. Fig. 9. Small tilted frustule showing broad fascia, radiate striae and deep mantle shallower near the apices. Fig. 10. Frustule in girdle view. Note girdle bands are missing. Fig. 11. Frustule tilted showing the valve view of the hypovalve. Fig. 12. Frustule tilted showing the epivalve. Note valve surface curved proximal region and vertical distal unperforated region of the mantle. Internal elliptical apertures are located at the junction of the valve face and mantle (arrowheads). Fig. 13. Frustule in girdle view. Note alveolate striae continuing shortly onto the valve mantle. Fig. 14. Frustule tilted showing the hypovalve and the mantle of the epivalve. Note excavated raphe fissures bent toward the margin of the valve in the same direction with terminal raphe fissure. Fig. 15. Detail of the polar region of a frustule in girdle view showing terminal raphe fissure finished near the valve margin (arrows). Scale bar: 10 µm in Figs 9–14; 5 µm in Fig. 15.

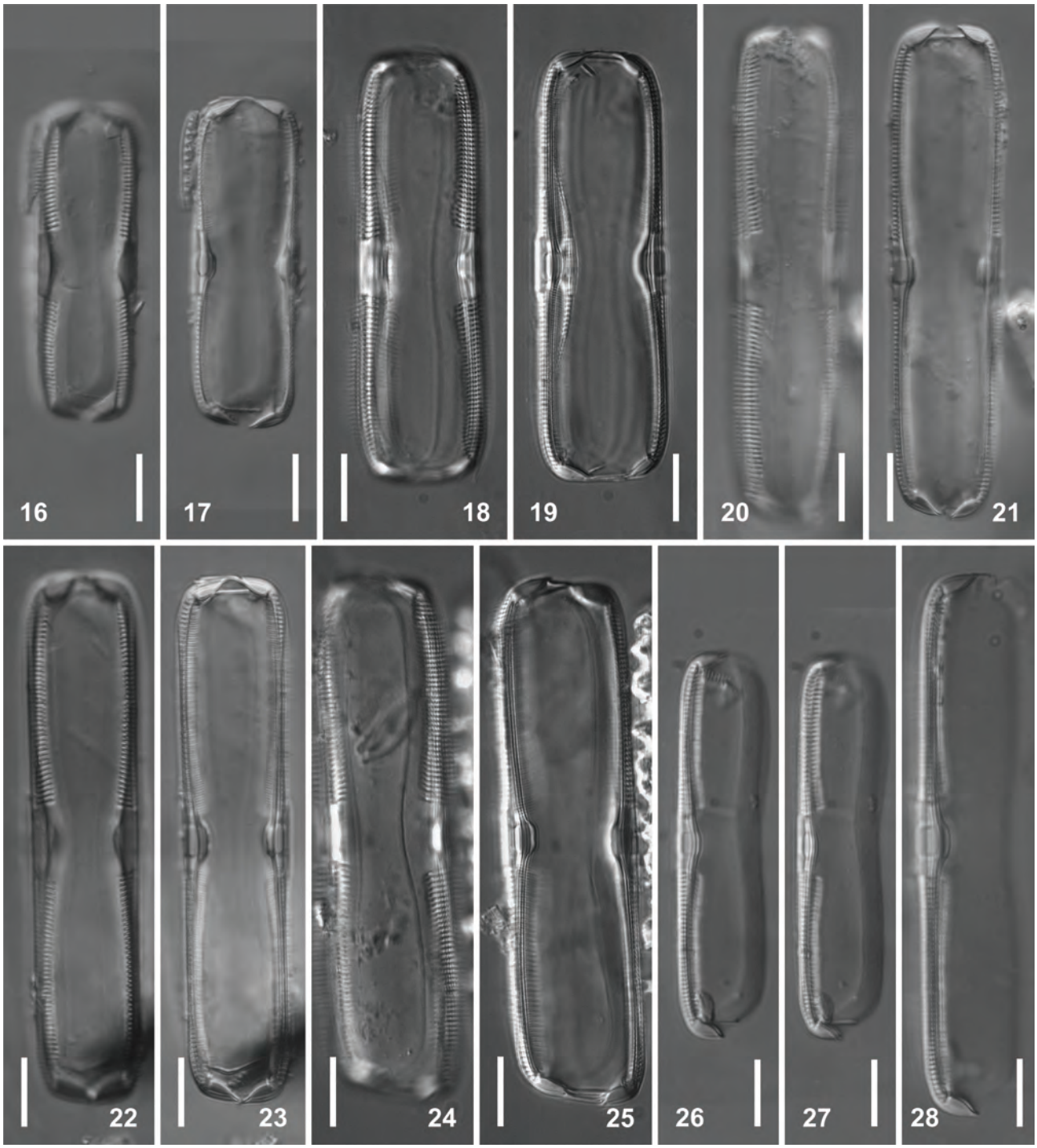

FIGURES 16–28. *Caloneis mendosina* Frenguelli (emend. Sar & Sunesen) from syntype material of *C. quilinesis*. LM. Figs 16–25. Frustules in girdle view, note obliquely reinforced corners. Figs 26–28. Valves in lateral view showing deep mantles. Scale bars: 10 µm.

Material and Methods

The original material of *Caloneis mendosina*, *C. mendosina* var. *minor* and *C. quilinensis* was obtained from the Frenguelli Collection deposited at the Herbarium of the División Ficología 'Dr. Sebastián A. Guarrera' (LPC), Facultad de Ciencias Naturales y Museo, Universidad Nacional de La Plata, Argentina. According to Frenguelli (1934, Table: 341) *C. mendosina* var. *mendosina* and *C. mendosina* var. *minor* were scarce and rare respectively in the slides of series # 319. In the case of *C. quilinensis*, Frenguelli & Cordini (1937, Table: 86) reported the species as rare in the slides of series # 306, scarce in the slides of series # 309 and frequent in the slides of series # 310.

Observations of the fifteen slides from series # 319 and the five slides from series # 310 with accompanying photomicrographs were made in light microscopy (LM) using a Leica DM 2500 (phase contrast and differential interference contrast; Leica Microsystems, Wetzlar, Germany) and a Zeiss Axiovert 40 CFL (phase contrast and DIC interference contrast; Zeiss Microimaging, Göttingen, Germany). Oxidized material from sample # 319 and # 310, present in the Frenguelli Collection (Sar *et al*. 2009, Table 1), was prepared for scanning electron microscope (SEM) using methods described by Ferrario *et al*. (1995) and observations were made with a Jeol JSM 6360 LV (JEOL, Tokyo, Japan). Morphological features of the taxa are illustrated by photomicrographs generated at the same scale to facilitate comparisons.

Terminology used to describe morphological features follows that recommended by Ross *et al*. (1979), Round *et al*. (1990) and Cox (2012).

TABLE 1. Comparison of the morphometric and morphologic data between syntype material of *Caloneis mendosina* and *C. quilinensis*. Abbreviations: nd, no data; *, observed from literature pictures.

Feature	**Frenguelli (1934) *Caloneis mendosina* var. *mendosina* and var. *minor***	**Slides of the series # 319 *Caloneis mendosina* var. *mendosina* and var. *minor***	**Frenguelli in Frenguelli & Cordini (1937) *Caloneis quilinensis***	**Slides of the series # 310 *Caloneis quilinensis***
Frustule shape	rectangular	rectangular, obliquely reinforced	rectangular	rectangular, with rounded corners, obliquely reinforced
Frustule height	15–36 µm	13–29 µm (n = 11)	*21 µm	7–18 µm (n = 49)
Original material analyzed in this study	13 µm			
Valve outline	panduriform	linear-panduriform, with barely gibbous central margin	linear, with triundulated margin	linear-elliptic, with triundulated margin, to linear-panduriform with barely gibbous central margin
Valve length	81–190 µm	46–106 µm (n = 14)	39–117 µm	39–81 µm (n = 95)
Original material analyzed in this study	58–64 µm			
Valve width	14–21 µm	9–14 µm (n = 7)	9–18 µm	7.5–16.0 µm (n = 25)
Original material analyzed in this study	12 µm			
Valve surface	nd	flat, narrow, gently depressed in the central area and slightly raised toward the poles, merging gently into a deep mantle	convex	flat, narrow, gently depressed in the central area and slightly raised toward the poles, merging gently in a deep mantle
Valve mantle	nd	deep, much shallower near the apices, with a very wide unperforated distal region	nd	deep, much shallower near the apices, with a very wide unperforated distal region
Apices	cuneate to apiculate	broadly apiculate to cuneate, slightly protracted	cuneate	cuneate to broadly apiculate, slightly protracted
Pseudosepta	nd	present and short, only seen in LM	nd	present and short seen in LM and SEM
Striae		alveolate, radiate, continuing shortly onto the mantle		idem

...continued on the next page

TABLE 1. (Continued)

Feature	Frenguelli (1934) *Caloneis mendosina* var. *mendosina* and var. *minor*	Slides of the series # 319 *Caloneis mendosina* var. *mendosina* and var. *minor*	Frenguelli in Frenguelli & Cordini (1937) *Caloneis quilinensis*	Slides of the series # 310 *Caloneis quilinensis*
Stria density	9–10 in 10 μm	11–15 in 10 μm (n = 14)	10–12 in 10 μm	13–16 in 10 μm (n = 87)
Type material analyzed in this study	11 in 10 μm			
Axial area	linear-lanceolate	lanceolate, narrow near the apices and gradually widening toward the central area	linear-lanceolate, narrow in smaller specimens and wider in bigger specimens	fusiform lanceolate, narrow near the apices and gradually widening toward the central area
Central area	*widened transapically forming a fascia	widened transapically forming a fascia	*widened transapically forming a fascia	widened transapically forming a fascia
External central raphe fissures	nd	dug out on the central area and ended in drop-like pores	nd	dug out on the central area and ended in drop-like pores
External polar raphe fissure	nd	deflected in the same direction as a continuous arch to one side of the apex and finished close to the margin of the mantle	nd	deflected in the same direction as a continuous arch to one side of the apex and finished close to the margin of the mantle
Internal central raphe endings	nd	nd	nd	absent or not visible
Internal terminal raphe endings	nd	nd	nd	ended distally in small helictoglossae
Girdle bands	pleuras with filiform rib forming a clepsydra nd	nd	nd	two, open valvocopula with a row of poroids, segmental copula, wide, unstructured

Results

Slides of the series #319 referenced by Frenguelli (1934) in the protologues of *Caloneis mendosina*, *Caloneis mendosina* var. *minor* and slides of the series # 310 referenced by Frenguelli in Frenguelli & Cordini (1937) in the protologue of *Caloneis quilinensis*, may be considered respective syntype materials according with Art. 9.5 of the ICN (McNeill *et al*. 2012). Unmounted material conserved in the Frenguelli Collection under the numbers #319 and #310 from which the slides of both series were mounted, was also part of the gathering, and used in this study for SEM analysis of the taxa.

Class Bacillariophyceae Haeckel emend. Medlin & Kaczmarska (2004)

Subclass Bacillariophycidae D.G. Mann in Round *et al.* (1990)

Order Naviculales Bessey emend. D.G. Mann in Round *et al.* (1990)

Family Pinnulariaceae D.G. Mann in Round *et al.* (1990)

Genus *Caloneis* Cleve (1894)

***Caloneis mendosina* Frenguelli (slides of series #319 and associated unmounted material) (Figs 1–15, Table 1)**
According to Frenguelli (1934) the nominal variety of *C. mendosina* and the var. *minor* differ by dimensions, valvar outline and stria density. The ranges of length of the valves given in the protologue were 81–190 μm for *C. mendosina*

var. *mendosina* and 58–64 µm for *C. mendosina* var. *minor*. Nevertheless, in the original material we found a continuous range of valve lengths between 46 and 106 µm (n = 14) and also a continuous range of stria density between 11 and 14 striae in 10 µm (n = 14). Larger specimens as those described by Frenguelli were not found in the analyzed material and the stria density was consistently higher than described by Frenguelli (1934, Table 1). All analyzed specimens showed rectangular frustules, 13–29 µm in depth (n = 9), with obliquely reinforced corners, almost always lying in girdle view (Figs 1–5, 10, 13). The valves are linear-panduriform in outline, with the central undulation narrower than the distal undulations, and broadly apiculate apices which are slightly protracted (Figs 6–8, 11). Small specimens are less panduriform, with cuneiform apices (Fig. 9). Valve length 46–106 µm (n = 14), valve width 9–14 µm (n = 7). The valve face is flat, narrow, depressed in the central area and slightly raised toward the poles (Figs 11, 12), merging gently into a deep mantle. The valve mantle, with a curved proximal region and a vertical distal region, is deep, much shallower near the apices, and mostly unperforated (Figs 1–5, 9–13). The overlap between valve mantles of the epivalve and hypovalve forms the figure of a clepsydra as described by Frenguelli in the protologue of the nominal variety (Figs 2, 5). The central nodule is elliptical, asymmetric (Figs 1–8). The axial area is lanceolate, narrow near the apices and distinctly widened toward the central area (Figs 8, 11, 12, 14). The central area is large, forming a symmetrical, broad fascia (Figs 3–14). The striae are alveolate, radial throughout the valve (Figs 6–9, 11, 12, 14), 11–14 in 10 µm (n = 14), and ending shortly onto the mantle (Figs 10, 13, 15). The outer layer of each alveolate stria appears eroded in all found specimens and the inner ingrowths of silica are opened by an elliptical aperture located at the apical junction of valve face and mantle (Figs 11, 12, 14, 15, arrowheads). The raphe is filiform, with slightly curved branches deflected in the same direction as the central fissures (Figs 8, 9, 11, 12, 14). The central fissures are distantly spaced, dug out on the central area and end in expanded drop-like pores, and weakly unilaterally bended toward one margin of the valve (Figs 6–8, 11, 12, 14). The terminal raphe fissures on the external face are deflected in the same direction, as a continuous arch to one side of the apex finishing close to the valve margin (Figs 14, 15). The girdle bands were absent in the analyzed material (Figs 9–15), possibly due to the oxidizing treatment. Taking into account the continuous range of size and stria density, and the ultrastructural similarities between smallest and largest specimens, we consider both taxa to be conspecific. Thus, we recommend that *Caloneis mendosina* var. *minor* should be considered a heterotypic synonym with *Caloneis mendosina*.

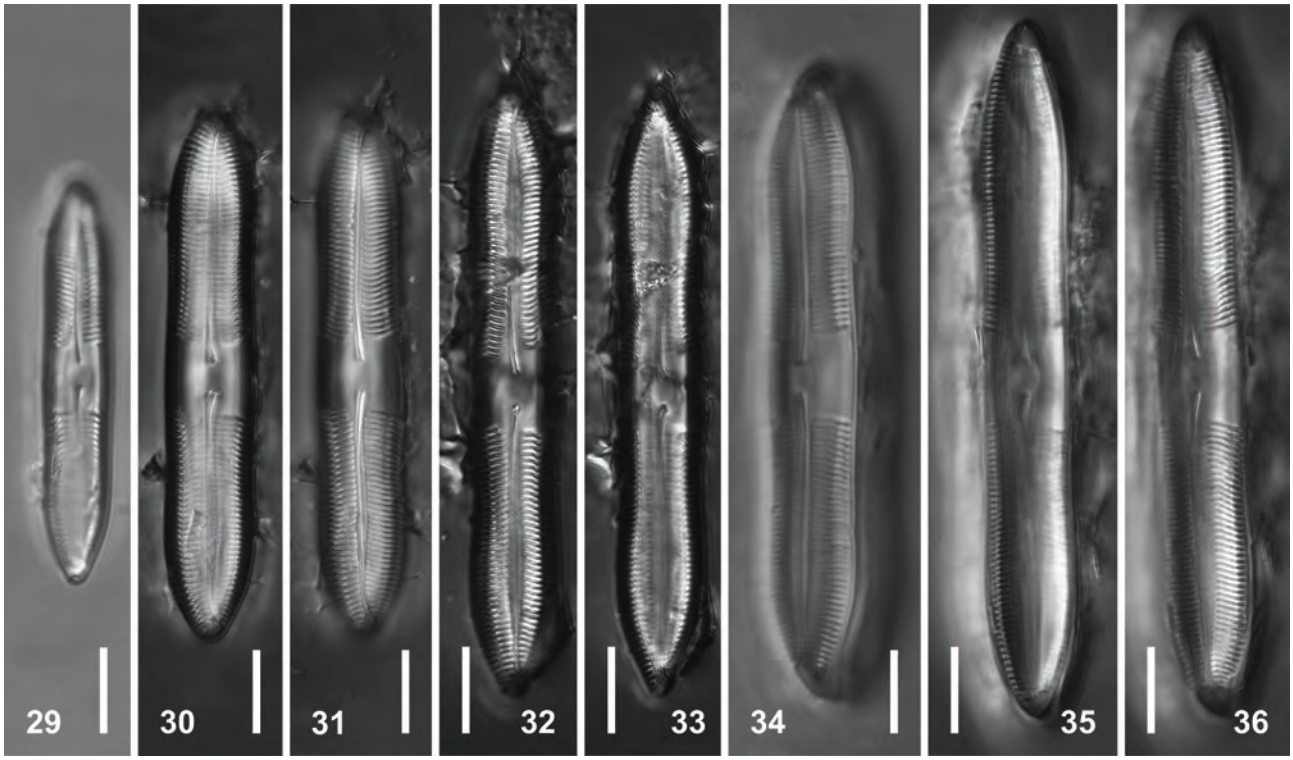

FIGURES 29–36. *Caloneis mendosina* Frenguelli (emend. Sar & Sunesen) from syntype material of *C. quilinesis*. LM. Figs 29–33. Valves linear-elliptic with triundulated margin to linear panduriform, note that distal undulations are wider than central undulation. Figs 30–31. The same specimen in different foci. Idem for figures 32–33. Fig. 34. Tilted frustule showing the hypovalve surrounded by the valvocopula. Figs 35–36. Different foci of a valve. Scale bars: 10 µm.

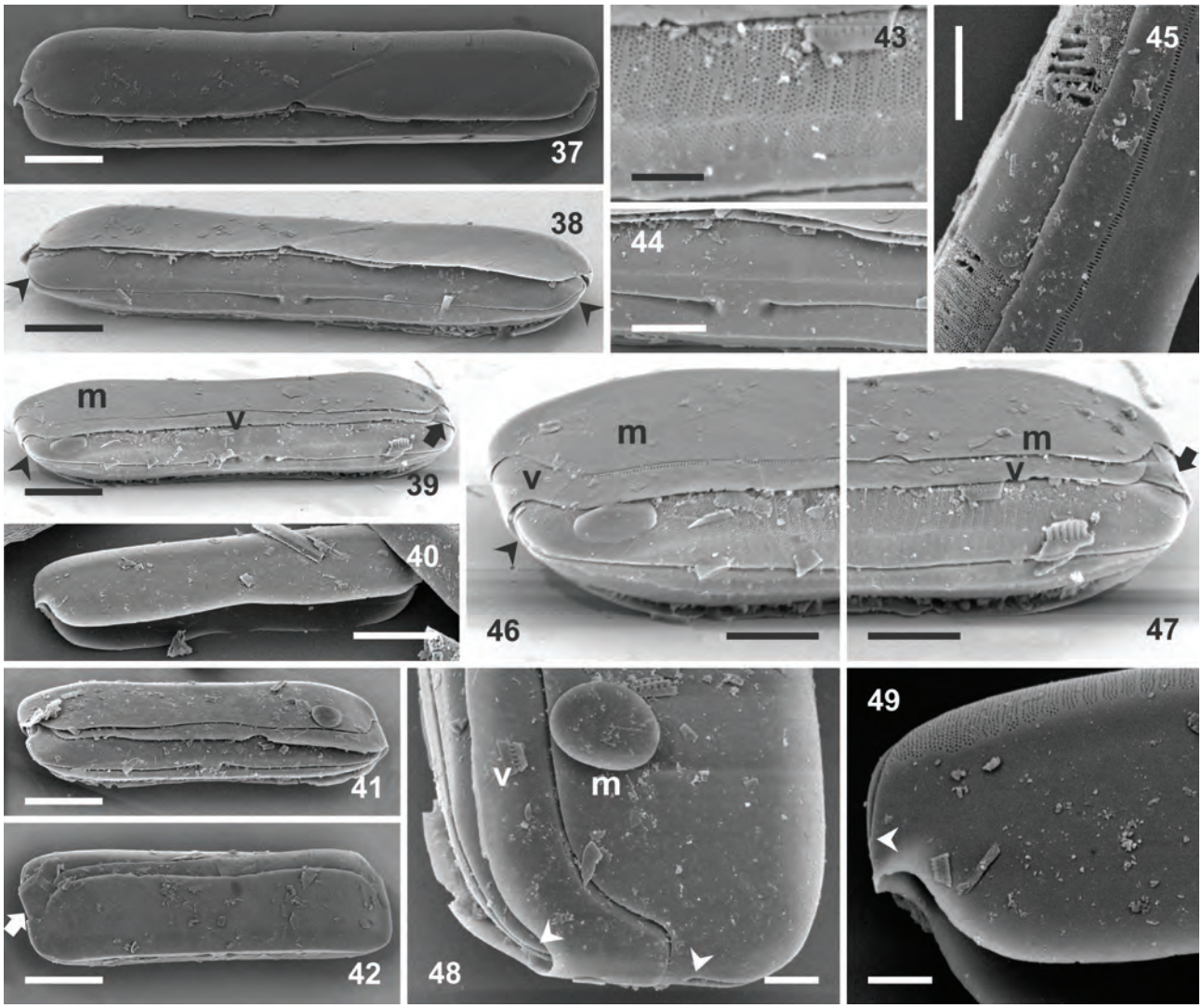

FIGURES 37–49. *Caloneis mendosina* Frenguelli (emend. Sar & Sunesen) from unmounted syntype material of *C. quilinesis.* SEM. External views. Arrowheads show terminal raphe fissures and arrows segmental copula. Figs 37–38. Same frustule in connective view and valvar view respectively. Fig. 39. Frustule showing the hypovalve and the epicingulum. Note vertical, unperforated region of the valve mantle of the epivalve, an open valvocopula and a segmental copula, m: mantle, v: valvocopula. Fig. 40. Valve in lateral view showing vertical, unperforated region of the valve mantle, shallower near the apices. Fig. 41. Frustule tilted similar to figure 39. Fig. 42. Frustule in girdle view. Note open valvocopula and segmental copula. Fig. 43. Detail of the figure 39 showing alveolae with outer areolate, multiseriate layer (3–4 poroids rows). Fig. 44. Detail of figure 32 showing central external raphe fissures dug out on the central area, ending in drop-like pores, deflected toward one side of the valve. Fig. 45. Detail of a central area showing alveolate striae of the hypovalve and valvocopula of the epicingulum with a row of elongate poroids. Figs 46–47. Detail of both apices of the valve in figure 39 showing the epicingulum, m: valve mantle, v: open valvocopula, and a segmental copula. Fig. 48. Detail of the polar area of a frustule in figure 41, note external terminal raphe fissure terminates close the valve margin (arrows). Fig. 49. Detail of a polar area of a valve in figure 40 showing the raphe fissure. Note alveolate striae continuing shortly onto the valve mantle. Scale bar: 10 μm in Figs 37–42; 5 μm in Figs 44–47; 2 μm in Figs 43, 48, 49.

Caloneis quilinensis **Frenguelli (slides of series #310 and associated unmounted material) (Figs 16–54, Table 1)**
Specimens observed were slightly shorter and narrower and had a higher stria density than those described in the protologue of Frenguelli in Frenguelli & Cordini (1937: 96) (Table 1). They all have rectangular frustules, with rounded, obliquely reinforced corners, almost always lying in girdle view, 8–18 μm in depth (n = 49) (Figs 16–25, 37, 42). The valves are linear-elliptic to linear-panduriform with a triundulated margin; the central undulation is slightly narrower than the distal undulations and the apices are cuneate to broadly apiculate (Figs 29–36, 50, 51). Valve length 39–81 μm (n = 95), valve width 7.5–16.0 μm (n = 25). The valve face is flat, narrow, gently depressed in the central area and slightly raised toward the poles (Figs 38, 39, 50, 51), merging gently into a deep mantle. The valve mantle, with a

curved proximal region and a vertical distal region, is deep, much shallower near the apices, and mostly unperforated (Figs 26–28, 40, 48, 49, 52). The overlap between the valve mantles forms the figure of a clepsydra (Figs 18, 19). The central nodule is elliptical, asymmetric (Figs 32, 35, 53). The axial area is fusiform-lanceolate, narrow near the apices and gradually widening toward the central area (Figs 31, 32). The central area is large, forming an asymmetrical, broad fascia (Figs 29–36, 45). The raphe is filiform, with slightly curved branches deflected in the same direction as the central fissures. The central external raphe fissures are dug out on the central area and end in drop-like pores (Figs 30–32, 38, 39, 41, 44). The terminal external raphe fissures are deflected in the same direction as a continuous arch to one side of the apex (Figs 30, 31, 38, 39, 46), and finish close to the margin of the mantle (Figs 38, 39, 46, 48, 49, 52 arrowheads). Internally, the raphe is seen as continuous at the central area, slightly undulate near a subtle, asymmetrical, central nodule (Figs 50, 51, 53), and end distally in small helictoglossae (Fig. 54, arrowhead). Pseudosepta surrounding both poles are very short (Figs 50, 54, arrows). The striae are alveolate, continuing shortly onto the mantle (Figs 43, 45, 49). Each stria has an outer areolate layer, multiseriate (3–4 poroids rows) (Figs 43, 45–47, 49) and an inner ingrowth of silica opening by an elliptical aperture (Figs 50, 51, 53, 54). These apertures are aligned and located at the junction of valve face and mantle (Figs 50, 51). The girdle is composed of two bands. The valvocopulae is open at one pole (Figs 39, 41, 42, 46–48), with one row of elongate poroids in the pars exterior (Figs 45, 46). The copula is wide, segmental, unstructured, occupying the gap left at the pole that close the full circumference of the valve mantle (Figs 39, 42, 47, arrows).

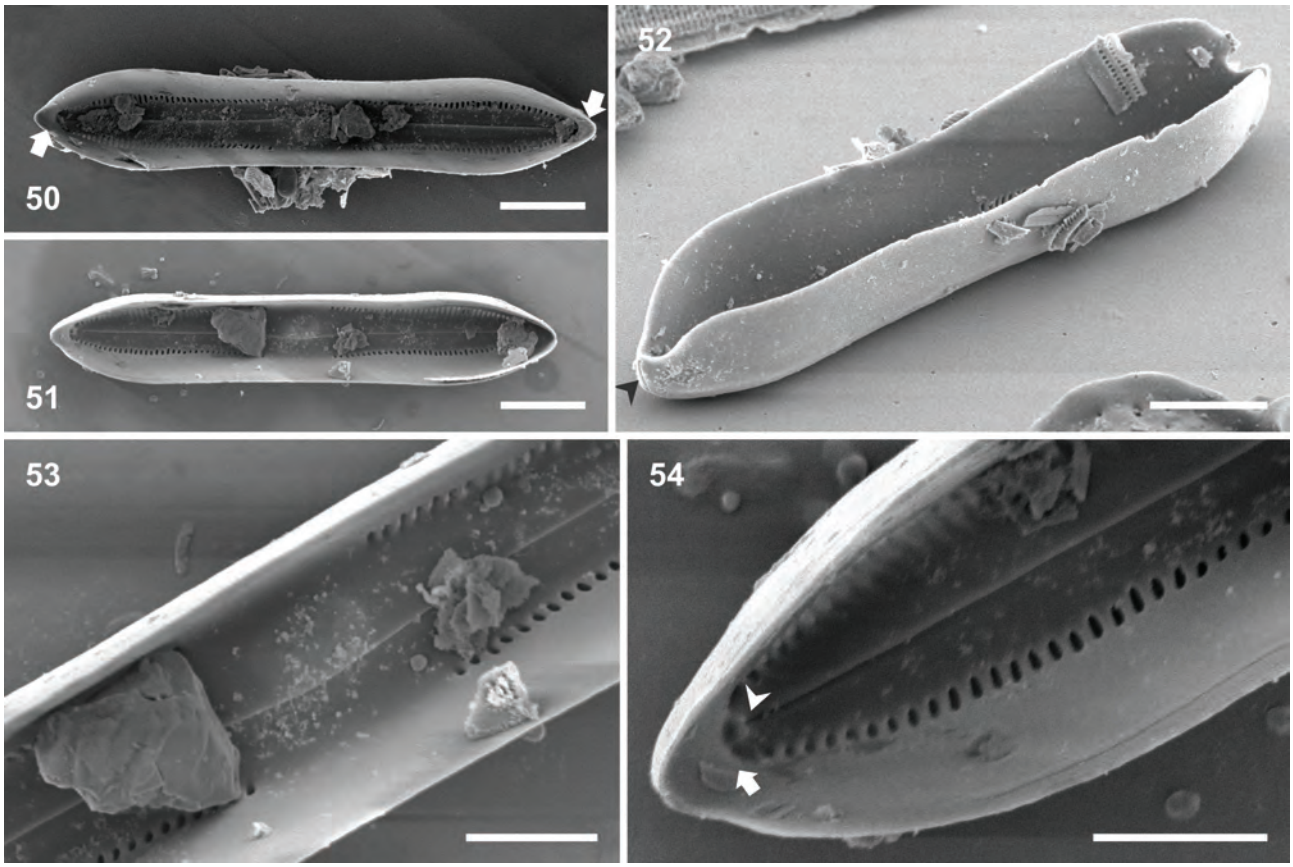

FIGURES 50–54. *Caloneis mendosina* Frenguelli (emend. Sar & Sunesen) from unmounted syntype material of *C. quilinesis.* SEM. Figs 50–51. Linear-panduriform valves with apiculate apices in internal view. Note the raphe is continuous at the central area and asymmetrical central nodule. Arrows show pseudosepta in figure 50. Fig. 52. Valve in lateral view showing valve mantle. Note terminal external raphe fissure finishing close to the valve margin (arrowhead). Fig. 53. Detail of the central nodule. Fig. 54. Detail of the apex of the valve in figure 51 showing a small helictoglossa (arrowhead) and a short pseudoseptum (arrow). Scale bar: 10 µm in Figs 50–52; 5 µm in Figs 53, 54.

Comparison of syntype material between taxa (Table 1)

Frenguelli in Frenguelli & Cordini (1937) explicitly compared *Caloneis quilinensis* with *Caloneis mendosina* establishing that they do not agree in details of shape and structure. Syntype material of *Caloneis mendosina* differs from that of *C. quilinensis* by higher dimensions and valves commonly linear-panduriform with broadly apiculate apices. However, the combined length and width ranges for these taxa form a potential diminution continuum. Additionally, some bigger specimens of *C. quilinensis* in the syntype material also present linear panduriform valves with apiculate apices, similar to smaller specimens of *C. mendosina* found in other syntype material.

The ultrastructural analysis of both species revealed numerous common features between them such as: 1) rectangular shape of frustules with remarkably reinforced angles; 2) shape of the valve surface, narrow lanceolate around the axial area an merging gently into the mantle; very deep valve mantle with a curved proximal region and a vertical distal region, and shallower at poles; 3) lanceolate to fusiform-lanceolate axial area, narrow near the apices and gradually widening toward the central area; 4) large central areas, forming an asymmetrical, broad fascia; 5) morphology and position of the raphe, with slightly curved branches deflected in the same direction; 6) size and position of the apertures of the alveolate striae which are elliptic, small, and placed at the junction of the valve surface and mantle.

Based on morphological comparisons and taking into account that both species come from similar diatomaceous earth deposits accompanied by several common freshwater species, we consider these taxa to be conspecific. Thus, we propose that the correct name of the species should be *Caloneis mendosina* Frenguelli emended Sar & Sunesen and *Caloneis quilinensis* should be considered as an heterotypic synonym.

Discussion

Taxonomic-nomenclatural changes proposed in this study

Caloneis mendosina Frenguelli 1934 (emended Sar & Sunesen)

REFERENCE: Frenguelli 1934, *Contribución al conocimiento de las diatomeas argentina. VIII Diatomeas del Pleistoceno Superior de las Guayquerías de San Carlos (Provincia de Mendoza). Revista del Museo de La Plata 34: 351, pl. 1, figs 9–11.*

HETEROTYPIC SYNONYM: *Caloneis mendosina* var. *minor* Frenguelli 1934, *Contribución al conocimiento de las diatomeas argentinas. VIII Diatomeas del Pleistoceno Superior de las Guayquerías de San Carlos (Provincia de Mendoza). Revista del Museo de La Plata 34: 351, pl. 1, fig. 12.*

HETEROTYPIC SYNONYM: *Caloneis quilinensis* Frenguelli in Frenguelli & Cordini 1937, *La diatomita del Quilino (Provincia de Córdoba). Su contenido y sus posibilidades de explotación. Revista del Museo de La Plata (n. s.) 1, Geología 2: 96, pl. 3, figs 14–18.*

LECTOTYPE: Slide LPC – 319 (2), here designated according the Art. 9.1 McNeill *et al*. (2012), labeled "lectotipo de *Caloneis mendosina*, (deposited in the Herbarium of the División Ficología "Dr. Sebastián A. Guarrera") (Figs 3, 4, 7, 8).

TYPE LOCALITY: Guayquerías of the Seco del Agua Salada River, Provincia de Mendoza, Argentina.

DESCRIPTION: Frustules rectangular, with rounded, obliquely reinforced corners, almost always lying in girdle view, 7–36 µm in depth. Valves linear-panduriform with barely gibbous central margin and broadly apiculate apices, to linear-elliptic with triundulated margin and cuneate apices, distal undulations wider than central undulation. Valve length 39–190 µm, valve width 7.5–21 µm. Valve face flat, narrow, gently depressed in the central area and slightly raised toward the poles, merging gently into a deep mantle. Valve mantle, with a curved proximal region and a vertical distal region, shallower near the apices, with a very wide unperforated distal region. Central nodule elliptical, asymmetric. Axial area fusiform-lanceolate, narrow near the apices and more or less gradually widening toward the central area. Central area large, forming an asymmetrical, broad fascia. Raphe filiform, with slightly curved branches deflected in the same direction. Central external raphe fissures, dug out on the central area and ending in drop-like pores, deflected toward one side of the valve. Terminal external raphe fissures deflected toward one side of the apex, ending close to the margin of the mantle. Internally, raphe continuous at the central area, slightly undulate near the central nodule, and distally ending in small helictoglossae. Pseudoseptum short present at both poles. Radial alveolate striae, continuing shortly onto the mantle. Stria density 10–16 in 10 µm. Alveoli with outer areolate, multiseriate layer (3–4 poroids rows) and inner ingrowths of silica opening by an elliptical aperture. Apertures aligned and located at the junction of valve face and mantle. Girdle composed of two bands, an open valvocopula with a row of elongate poroids in the pars exterior and a wide and unstructured segmental copula.

DISTRIBUTION IN ARGENTINA: *Caloneis mendosina* is a fossil, freshwater species, from a Guayquerías Pleistocene deposit, located in the Seco del Agua Salada River, Province of Mendoza and from, a Quilino "Holocene" deposit, located in the Province of Córdoba.

TABLE 2. Comparison of the morphometric and morphologic data between *Caloneis mendosina* Frenguelli (emend. Sar & Sunesen) and allied species. Abbreviations: nd, no data; *, observed from literature pictures.

Feature	*Caloneis mendosina* Frenguelli (emend. Sar & Sunesen)	*Caloneis silicula* (Ehrenberg) Cleve f. *peisonis* (Grunow) Krammer in Krammer & Lange-Bertalot	*Caloneis columbiensis* Cleve	*Caloneis nipponica* Skvortzow	*Caloneis laticingulata* Metzeltin, Lange-Bertalot & García-Rodríguez
Reference	This study	Cocquyt (1999: 427, figs 1–8, 24, 26–29)	Cleve (1894: 51, pl. 3, fig. 4), Metzeltin *et al*. (2005 pl. 153, 12–14)	Skvortzow (1936: 267, pl. 2, fig. 7, pl. 3, fig. 9, pl. 4, fig. 15), Ohtsuka & Tuji (2002: 244, figs 1, 2)	Metzeltin *et al*. (2005: 29, pl. 156, figs 1–8)
Frustule shape	rectangular, with more or less rounded corners, obliquely reinforced	rectangular*	nd	nd	rectangular, with corners obliquely reinforced
Frustule height	7–36 µm	nd	nd	nd	30–35 µm
Valve outline	linear-elliptic, with triundulated margin, to linear-panduriform with barely gibbous central undulation narrower than distal undulation	linear-elliptic, with triundulated margin, to linear-panduriform with central undulation wider than distal undulation	linear-panduriform with triundulate margin, central undulation wider than distal undulations	linear-panduriform with triundulate margin, central undulation narrower than distal undulations	linear lanceolate with a central undulation
Valve length	39–190 µm	40–77.5 µm	44 µm	42–60 µm	75–95 µm
Valve width	7.5–21 µm	10.5–12.5 µm	7 µm	7–10 µm	9.5–10.5 µm
Valve surface	flat, narrow, gently depressed in the central area and slightly raised toward the poles, merging gently in a deep mantle	flat, with two shallow depressions parallel to the raphe, curving abruptly in a deep valve mantle	nd	nd	nd
Valve mantle	deep, much shallower near the apices, with a curved proximal region and a wide vertical distal region, unperforated	deep, slightly shallower near the apices	nd	nd	deep, very shallower near the apices
Apices	cuneate to broadly apiculate, slightly protracted	cuneate	cuneate to apiculate, not protracted	broadly truncate with rounded to apiculate ends	cuneate
Pseudoseptum	present and short seen in LM and SEM	nd	nd	nd	probably present
Striae	alveolate, radiate throughout the valve, continuing shortly onto the mantle	alveolate, radiate, always visible near the valve margins, sometimes extended up to raphe	straight towards the distal undulations becoming radial at the apices	radiate throughout the valve	radiate throughout the valve, continuing shortly onto the mantle
Stria density	10–16 in 10 µm	15–17 in 10 µm	19 in 10 µm	17–18 in 10 µm	12–13 in 10 µm

...continued on the next page

TABLE 2. (Continued)

Feature	*Caloneis mendosina* Frenguelli (emend. Sar & Sunesen)	*Caloneis silicula* (Ehrenberg) Cleve f. *peisonis* (Grunow) Krammer in Krammer & Lange-Bertalot	*Caloneis columbiensis* Cleve	*Caloneis nipponica* Skvortzow	*Caloneis laticingulata* Metzeltin, Lange-Bertalot & García-Rodríguez
Axial area	fusiform lanceolate to lanceolate, narrow near the apices and gradually widening toward the central area	broad, elliptical with LM, and narrower with SEM Striae finished in the shallower depression parallel to the raphe	fusiform lanceolate, narrow near the apices and gradually widening toward the central area		moderately broad, narrow near the apices and gradually widening toward the central area.
Central area	widened transapically forming a broad fascia	widened transapically forming a narrow fascia	widened transapically forming a narrow fascia	widened transapically forming a broad fascia	widened transapically forming a broad fascia
External central raphe fissures	dug out on the central area and ends in drop-like pores	somewhat enlarged and expanded, bent towards the valve mantle	enlarged and expanded, bent towards the valve mantle	somewhat enlarged and expanded, bent towards the valve mantle	somewhat enlarged and expanded, bent towards the valve mantle
External polar raphe fissure	deflected both in the same direction and in the same direction as the central ones, finished close to the margin of the valve-mantle	deflected both in the same direction and in opposite direction as the central ones, expanded on the valve-mantle	deflected both in the same direction and in opposite direction as the central ones, expanded on the valve-mantle	deflected both in the same direction and in the same direction as the central ones	deflected both in the same direction and in opposite direction as the central ones
Internal central raphe endings	absent or not visible	nd	nd	nd	nd
Internal terminal raphe endings	ended distally in small helictoglossae	nd	nd	nd	nd
Girdle bands	two, open valvocopula with a row of poroids, segmental copula, wide, unstructured	two, open valvocopula with a row of poroids, segmental copula, wide, unstructured	nd	nd	nd

Comparison of *Caloneis mendosina* with morphologically related species (Table 2)

Caloneis mendosina is similar to *C. silicula* and associated varieties based on the observations of Cleve (1894). Krammer & Lange-Bertalot (1986) revealed that the most similar taxon to *Caloneis mendosina* is *C. silicula* f. *peisonis* (Grunow) Krammer in Krammer & Lange-Bertalot (1985: 22; 1986: 88, pl. 172, fig. 8). The comparison between the LM figures of both taxa shows that they have similar valve forms, e.g., linear-elliptic to linear-panduriform with triundulated outline, and apices are cuneate; nevertheless, the central undulation is narrower than distal undulations in *C. mendosina* and wider in *C. silicula* f. *peisonis* (Table 2). SEM illustrations of *C. mendosina* and *C. silicula* f. *peisonis* (Cocquyt 1999: 427, figs 1–8, 24, 26–29) provide more information on similarities and differences between the two taxa. Both taxa are similar in having a deep valve mantle, robust and narrower toward the poles and two girdle bands, an opened valvocopula and a segmental copula (Cocquyt 1999: figs 26–29). Nevertheless, in *C. mendosina* the valve surface is narrow and flat with a curved proximal region and a vertical distal region merging gently into a deep mantle, while in *C. silicula* f. *peisonis* the valve surface is wide and flat curving abruptly into a deep mantle. This causes the frustules of *C. mendosina* to orientate in girdle view, while frustules of *C. silicula* f. *peisonis* are commonly lying in valve view. Also the terminal and central raphe fissures are slightly curved, deflected in the same direction in *C. mendosina*, whereas in opposite directions in *C. silicula* f. *peisonis*.

Other two freshwater species that show similarities with *Caloneis mendosina* are *C. columbiensis* Cleve (1894: 51, pl. 3, fig. 4) described from Columbia River and *C. nipponica* Skvortzow (1936: 267, pl. 2, fig. 7, pl. 3, fig. 9, pl. 4, fig. 15) described from diatom clay of Biwa Lake. They are similar in the linear-panduriform, triundulated valve outline. *C. columbiensis* pictured by Cleve (1894) and Metzeltin *et al*. (2005, figs 12–14) differs from *C. mendosina* in having the central undulation wider than the distal undulations; denser striae, straight toward the distal undulations

becoming radial at the apices; and relatively narrower fascia barely longer than the central nodule (Table 2). *Caloneis nipponica* pictured by Skvortzow (1936) and lectotypified by Ohtsuka & Tuji [2002: 244, figs 1, (Lectotype, slide 30000136), 2] also agree with *C. mendosina* in having a central undulation narrower than distal undulations, broad fascia, striae radiate throughout the valve and terminal external raphe fissures deflected toward one side of the apex in the same direction as the central external raphe fissure (Table 2). Both taxa show subtle differences in stria density, 17–18 in 10 µm in *C. nipponica* vs 10–16 in 10 µm for *C. mendosina*. Unfortunately, LM and SEM descriptions of the frustule in girdle view are not available for *Caloneis nipponica*, thus a comparison cannot be completed. However, considering that *C. mendosina* was erected earlier than *C. nipponica* the ultrastructural analysis of the later was not imperative for determining the correct epithet of the taxon and was beyond the scope of this study.

Despite the fact that not many species in the genus *Caloneis* have been analyzed with SEM, it is possible to detect two groups of species with triundulated outline based on the depth of the valve mantle. One group including the species *C. fasciata* (Lagerstedt) Cleve (pictured by Antoniades *et al*. 2009, figs 4–6), *C. fusus* Hamilton & Antoniades in Antoniades *et al*. (2009, figs 50–58), *C. schumanniana* (Grunow) Cleve and *C. lewisii* Patrick (pictured by Stancheva *et al*. 2009, figs 39–42 and 43, 44 respectively) is characterized by a shallow valve mantle almost regular in depth around the valve. The second group includes *C. australis* Zidarova, Kopalová & Van de Vijver (2016: 40, figs 13–17), *C. mendosina* (this study), *C. silicula* f. *peisonis* (pictured by Cocquyt 1999, figs 26–29) and is characterized by having a deep valve mantle, slightly or abruptly shallower at the apices. Among the mentioned species *C. mendosina* is the only one that shows a mantle with curved proximal region and vertical distal region.

Caloneis laticingulata Metzeltin, Lange-Bertalot & García-Rodríguez (2005: 29, pl. 156, figs 1–8) was described based on LM. Metzeltin *et al*. (2005, fig. 8) shows that this species clearly belongs to the second group and is similar with *C. mendosina* having a broad girdle, reinforced angles, and a clepsydra shape due to the overlapping of epivalve and hypovalve mantles and valvocopulae. However, *C. laticingulata* can be distinguished from *C. mendosina* by the valve outline, linear lanceolate with a central undulation and cuneate apices, and by the central and terminal external raphe fissures bent in opposite directions (Table 2).

Prospects for future studies of *Caloneis*

The difficulties in determining species of the genus *Caloneis* are due to the scarcity of available SEM images resulting in poor knowledge of valve and frustule ultrastructure; the similarity in valve outline and dimensions among numerous species; the intraspecific morphological variability of some species; and poor original descriptions. It is thus necessary to study by scanning electron microscopy the type material of *C. silicula*, its intraspecific taxa, and other species with a linear elliptic outline and a central undulation, such as *C. laticingulata*. It is also necessary to examine species with panduriform outlines such as *C. nipponica*, for an accurate determination of frustule morphology, boundary of the valve face and mantle, morphology of the mantle, and presence or absence of fascia on valve and morphology of the cingula.

Acknowledgements

Authors wish to thank to two anonymous reviewers for valuable comments which contributed to improve the manuscript. The research was supported by grants from the Universidad Nacional de La Plata 11/N722 and from the Consejo Nacional de Investigaciones Científicas y Técnicas, PIP0067.

References

Antoniades, D., Hamilton, P.B., Douglas, M.S.V. & Smol, J.P. (2007) *Diatoms of North America: The freshwater floras of Prince Patrick, Ellef Ringnes and northern Ellesmere Islands from the Canadian Arctic Archipelago.* [Iconographia Diatomologica 17] A.R.G. Gantner, Ruggel, 649 pp.

Antoniades, D., Hamilton, P.B., Hinz, F., Douglas, M.S.V. & Smol, J.P. (2009) Seven new species of freshwater diatoms (Bacillariophyceae) from the Canadian Arctic Archipelago. *Nova Hedwigia* 88: 57–80. https://doi.org/10.1127/0029-5035/2009/0088-0057

Cleve, P.T. (1894) Synopsis of the Naviculoid Diatoms, Part I. *Kongliga Svenska-Vetenskaps Akademiens Handlingar* 26: 1−194, 5 pls.

Cocquyt, C. (1999) Diatoms from a hot spring in Lake Tanganika. *Nova Hedwigia* 68: 425–439.

Cox, E.J. (2012) Ontogeny, homology, and terminology—wall morphogenesis as an aid to character recognition and character state definition for Pennate diatom systematics. *Journal of Phycology* 48: 1–31.
https://doi.org/10.1111/j.1529-8817.2011.01081.x

Ferrario, M.E., Sar, E.A. & Sala, S.E. (1995) Metodología básica para el estudio del fitoplancton con especial referencia a las diatomeas. *In:* Alveal, K., Ferrario, M.E., Oliveira, E.C. & Sar, E. (Eds.) *Manual de Métodos Ficológicos*. Universidad de Concepción, Concepción, pp. 1–23.

Frenguelli, J. (1923) Contribuciones para la sinopsis de las diatomeas argentinas. I Diatomeas del Río Primero en la ciudad de Córdoba. *Boletín de la Academia Nacional de Ciencias de Córdoba* 27: 13–119.

Frenguelli, J. (1934) Contribución al conocimiento de las diatomeas argentina. VIII Diatomeas del Pleistoceno Superior de las Guayquerías de San Carlos (Provincia de Mendoza). *Revista del Museo de La Plata* 34: 339–371.

Frenguelli, J. & Cordini, R. (1937) La diatomita del Quilino (Provincia de Córdoba). Su contenido y sus posibilidades de explotación. *Revista del Museo de La Plata (n. s.) 1, Geología* 2: 67–116.

Krammer, K. & Lange-Bertalot, H. (1985) Naviculaceae. Newe und wenig bekannte Taxa, newe Kombinationen und Synonyme sowie Bemerkungen zu einigen Gattungen. *Bibliotheca Diatomologica* 9: 1–213. [J. Cramer., Stuttgart]

Krammer, K. & Lange-Bertalot, H. (1986) Bacillariophyceae 1. Teil. Naviculaceae. *In:* Ettl H., Gerloff, J., Heynig, H. & Mollenhauer, D. (Eds.) *Süsswasserflora von Mitteleuropa (begründet von A. Pascher), Band 2/1*. Gustav Fischer, Stuttgart, 876 pp.

McNeill, J., Barrie, F.R., Buck, W.R., Demoulin, V., Greuter, W., Hawksworth, D.L., Herendeen, P.S., Knapp, S., Marhold, K., Prado, J., Prud'homme van Reine, W.F., Smith, G.F., Wiersema, J.H. & Turland, N.J. (2012) *International Code of Nomenclature for algae, fungi, and plants (Melbourne Code).* Koeltz Scientific Books, Koenigstein, 241 pp. Available from: http://www.iapt-taxon.org/nomen/main.php? (accessed 1 April 2017)

Medlin, L.K. & Kaczmarska, I. (2004) Evolution of the diatoms: V. Morphological and cytological support for the major clades and a taxonomic revision. *Phycologia* 43: 245−270.
https://doi.org/10.2216/i0031-8884-43-3-245.1

Metzeltin, D., Lange-Bertalot, H. & García-Rodríguez, F. (2005) *Diatoms of Uruguay. Compared with other taxa from South America and elsewhere.* [Iconographia Diatomologica 15] A.R.G. Gantner, Ruggel, 736 pp.

Ohtsuka, T. & Tuji, A. (2002) Lectotypification of some pennate diatoms described by Skvortzow in 1936 from Lake Biwa. *Phycological Research* 50: 243–249.
https://doi.org/10.1046/j.1440-1835.2002.00281.x

Ross, R., Cox, E.J., Karayeva, N.I., Mann, D.G., Paddock, T.B.B., Simonsen, R. & Sims, P.A. (1979) An amended terminology for the siliceous components of the diatom cell. *Nova Hedwigia, Beiheft* 64: 513–533.

Round, F.E., Crawford, R.M. & Mann, D.G. (1990) *The Diatoms. Biology and morphology of the genera*. Cambridge University Press, Cambridge, 747 pp.

Sar, E.A., Sala, S.E., Sunesen, I., Henninger, M.S. & Montastruc, M. (2009) *Catálogo de los géneros, especies y taxa infraespecíficos erigidos por J. Frenguelli/Catalogue of the genera, species and infraspecific taxa erected by Frenguelli.* [Diatom Monograph 10] A. R. G. Gantner, Ruggell, 419 pp.

Skvortzow, B.W. (1936) Diatoms from Biwa Lake, Honshu Island, Nippon. *Philippine Journal of Science* 61: 253–296, 8 pls.

Stancheva, R. Manoylov, K. & Gillett, N. (2009) Morphological variation of the *Caloneis schumanniana* species complex (Bacillariophyceae) from different environmental conditions in North American streams. *Hydrobiologia* 635: 157–170.
https://doi.org/10.1007/s10750-009-9908-4

Van Heurck, H. (1881) *Synopsis des Diatomées de Belgique*. Atlas pls. 31–77. [Ducaju et Cie, Anvers]

VanLandingham, S.L. (1978) *Catalogue of the fossil and recent genera and species of diatoms and their synonyms. Part* 7, *Rhoicosphenia through Zygoceros.* J. Cramer, Vaduz, pp. 3606–4241.

Zidarova, R., Kopalová, K. & Van de Vijver, B. (2016) Ten new Bacillariophyta species from James Ross Island and the South Shetland Islands (Maritime Antarctic Region). *Phytotaxa* 272: 37–62.
https://doi.org/10.11646/phytotaxa.272.1.2